

## Vaporization Rates, Surface Topography, and Vaporization Mechanisms of Single Crystals: A Case Study

Gerd M. Rosenblatt

*Department of Chemistry, The Pennsylvania State University, University Park, Pennsylvania 16802*

*Received September 8, 1975*

### The Role of Evaporation Kinetics

Investigations of the sublimation behavior of single crystals enable one to explore the molecular pathways by which atoms bound in a solid rearrange and escape to form free gaseous molecules. For this reason, vaporization is closely related to other surface reactions which involve a transition between a crystalline solid and a dilute fluid phase—such as electrolysis, dissolution, crystal growth, and heterogeneous catalysis. Such surface reactions usually proceed by a sequence of reaction steps: from an immobile (crystal) site, through a mobile surface-adsorbed state, to removal from the surface. In vaporization, dissolution, and electrolysis this sequence is traversed in the forward direction; in condensation and crystal growth, in the reverse direction. In corrosion, gas-surface reactions, and heterogeneous catalysis, the sequence is often traversed in both directions. Experimental studies of the vacuum vaporization of nearly perfect, elemental, single crystals allow examination of this reaction path under conditions which minimize complications caused by variations and uncertainties in surface and bulk composition, product vapor species, and surface structure. Thus, the kinetic role of surface defects such as dislocations, surface steps, and impurities may be ascertained in some detail.

The present Account describes the way in which detailed studies of evaporation from a prototype system—single-crystal arsenic—have provided considerable insight into the molecular processes occurring when gaseous molecules are formed from crystal atoms.

### Vaporization Coefficients and Retarded Vaporization

Vaporization rates are usually described by comparison with a maximum rate set by the equilibrium

vapor pressure,  $P_E$ , of the crystal.<sup>1-6</sup> The flux of vapor molecules incident upon a surface when the surface and vapor are at equilibrium in a closed container is  $P_E(2\pi mkT)^{-1/2}$ , where  $m$  is the mass of a vapor molecule. This is also the flux leaving the surface since, at equilibrium, these fluxes are equal. When a surface evaporates in vacuo, the vaporization flux  $J_v^\circ$  must be less than or equal to the flux of molecules which leave the same surface under equilibrium conditions:

$$J_v^\circ = \alpha_v^\circ P_E(2\pi mkT)^{-1/2} \quad (1)$$

The vacuum vaporization coefficient  $\alpha_v^\circ$  is less than or equal to 1.

Both theory and experiment show that  $\alpha_v^\circ$  is very close or equal to 1 upon evaporation of solids which form atomic vapors or which form gaseous species which preexist in the solid.<sup>1-7</sup> This is the basis of the Langmuir<sup>1</sup> method for the determination of vapor pressures in which the vapor pressure is calculated from the observed mass loss per unit time per unit area,  $r_L = \Delta w/A\Delta t$ , from a solid heated under vacuum.

$$P_L = r_L(2\pi kT/m)^{1/2} \quad (2)$$

However, solids which vaporize to form gaseous species which do not exist as such in the solid lattice, either because their formation requires covalent bond rearrangement or the disturbance of long-range electrostatic forces in ionic crystals, may have vaporization coefficients much less than one.<sup>2,4-6,8</sup> In this case, vaporization coefficients may be determined by comparing Langmuir vapor pressures,  $P_L$ , with equilibrium vapor pressures:

$$\alpha_v^\circ = P_L/P_E \quad (3)$$

(1) I. Langmuir, *Phys. Rev.*, **2**, 329 (1913).

(2) O. Knacke and I. N. Stranski, *Prog. Met. Phys.*, **6**, 181 (1956).

(3) J. P. Hirth and G. M. Pound, *Prog. Mater. Sci.*, **11**, 1 (1963), and earlier papers cited therein.

(4) G. A. Somorjai and J. E. Lester, *Prog. Solid State Chem.*, **4**, 1 (1967).

(5) A. W. Searcy in "Chemical and Mechanical Behavior of Inorganic Materials", A. W. Searcy, D. W. Ragone, and U. Colombo, Ed., Interscience, New York, N.Y., 1970, pp 107-133.

(6) G. M. Rosenblatt, *Treatise Solid State Chem.*, **6**, Chapter 3 (1976).

(7) G. M. Pound, *J. Phys. Chem. Ref. Data*, **1**, 135 (1972).

(8) L. Brewer and J. S. Kane, *J. Phys. Chem.*, **59**, 105 (1955).

Gerd M. Rosenblatt was born in Leipzig in 1933. His undergraduate work was done at Swarthmore College. Following receipt of the Ph.D. degree from Princeton University in 1960, he was a staff member at Lawrence Berkeley Laboratory until his appointment to the faculty of The Pennsylvania State University in 1963. His research interests are in the areas of gas-surface reactions and of high-temperature chemistry.

**Table I**  
Steady-State Vaporization Kinetics of  $\text{As}_4$  from  $\text{As}(111)$  at 550 K

Langmuir vapor pressure, $P_L$	$6.6 \times 10^{-10}$ atm
Vaporization coefficient, $\alpha_v^\circ$	$8.3 \times 10^{-5}$
Activation enthalpy, $\Delta H^*$	43.9 kcal
Excess activation enthalpy, $\Delta H^* - \Delta H^\circ$	8.6 kcal
Activation entropy, $\Delta S^*$	37.9 cal/deg
Excess activation entropy, $\Delta S^* - \Delta S^\circ$	-3.0 cal/deg

The temperature dependence of vaporization rates is often described by computing Langmuir vapor pressures,  $P_L$ , from the measured rates,  $r_L$ , and fitting the results to the expression<sup>6</sup>

$$-R \ln P_L = (\Delta H^*/T) - \Delta S^* \quad (4)$$

Equation 4 is analogous to the equilibrium thermodynamic relation

$$-R \ln P_E = (\Delta H^\circ/T) - \Delta S^\circ \quad (5)$$

When  $\alpha_v^\circ = 1$ , then  $\Delta H^* = \Delta H^\circ$  and  $\Delta S^* = \Delta S^\circ$ . Under these circumstances little can be learned, from measurements of vaporization rates, about the atomistic processes preceding desorption of vapor molecules from the surface.<sup>5,6,9</sup> However, if vaporization is retarded by chemical processes so that  $\alpha_v^\circ \ll 1$ , then  $\Delta H^* \neq \Delta H^\circ$  or  $\Delta S^* \neq \Delta S^\circ$  or both. Studies of such systems can yield mechanistic insight into the sequential steps in the vaporization process. In addition to its fundamental interest, the behavior of systems exhibiting retarded vaporization is of importance in various aspects of materials science.<sup>5</sup>

### Arsenic

Elemental arsenic represents a system for which  $\alpha_v^\circ \ll 1$ .<sup>8</sup> Kinetic results for the vacuum vaporization of  $\text{As}_4$  from  $\text{As}(111)$  single-crystal surfaces, under steady-state conditions, are summarized in Table I.<sup>10,11</sup> Tetrahedral  $\text{As}_4$  is the only important vapor species at moderate temperatures; its concentration exceeds that of gaseous  $\text{As}_2$  by a factor of  $10^4$  or more at 550 K.<sup>11,12</sup> The atomic rearrangement required to form  $\text{As}_4$  from the rhombohedral crystal lattice is shown schematically in Figure 1. The geometric rearrangement is accompanied by extensive changes in the electronic structure and chemical bonding. The data in Table I show that  $\alpha_v^\circ$  depends upon temperature and that most of the retardation of the vaporization rate of arsenic, by a factor of  $10^4$  near 550 K, is an energy effect. The excess activation entropy of -3 cal/deg corresponds to a reduction in rate by less than a factor of 5.

When freshly cleaved arsenic single crystals are first heated they sublime at rates below the steady-state rates shown in Table I. The present account is concerned primarily with the way in which investigations of the changes in rate and surface topography, which occur during this initial induction period, can yield insight into the molecular vaporization mechanism.

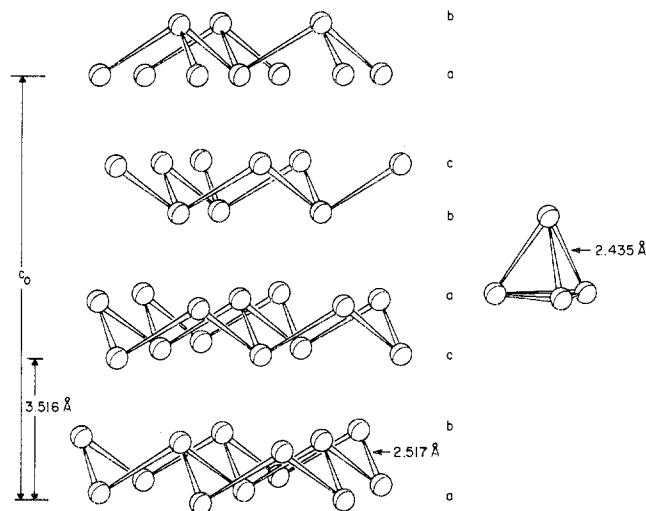


**Figure 1.** Crystal structure of arsenic compared to the geometry of gaseous  $\text{As}_4$ . The (111) surface is in a horizontal plane perpendicular to the page.

### Vaporization Rates and Morphological Changes during Induction Period

**Surface Features.** Changes in surface morphology, which occur upon evaporation, can be examined and measured continuously by vaporizing single crystals in a vacuum hot stage attached to an interference microscope. Figure 2 illustrates the changes observed upon evaporation of freshly cleaved arsenic.<sup>13-17</sup> The unevaporated (111) surface appears flat in the region between cleavage steps. When the crystal is heated, triangular pits appear on the surface. As vaporization proceeds, the pits grow until they intersect. These changes require net mass loss from the crystals and are not seen on crystals heated in sealed ampules.

Interferometry shows that pits are much too shallow for their sides to be composed of low-index crystallographic planes. Although the angles between pit sides and the (111) surface vary somewhat from crystal to crystal, typically handled crystals cleaved at room temperature form pits with slopes relative to (111) in the range 8 to 13°, average 11°.<sup>14-16</sup> The slopes of typical triangular pits remain constant as the pits grow. Triangular pit sides form flat planes with no measurable curvature.<sup>13</sup> Typical pit densities are  $5 \times 10^6 \text{ cm}^{-2}$ ,<sup>14</sup> the same order as dislocation densities. The pit slopes and densities suggest that pits form at the point where dislocation lines intersect the (111) surface. This conclusion is borne out by the observation that pits appear at high density in rows following strain lines and by examining pit formation and growth on surfaces which have been stressed locally (forming lines of dislocations) or which have been etched previously with a chemical shown by

(13) G. M. Rosenblatt in "Heterogeneous Kinetics at Elevated Temperatures", G. R. Belton and W. L. Worrell, Ed., Plenum Press, New York, N.Y., 1970, p 209.

(14) G. M. Rosenblatt, M. B. Dowell, P. K. Lee, and H. R. O'Neal in "The Structure and Chemistry of Solid Surfaces", G. A. Somorjai, Ed., Wiley, New York, N.Y., 1969, Chapter 38.

(15) J. W. Tester, C. C. Herrick, and R. C. Reid, *J. Appl. Phys.*, **44**, 1968 (1973).

(16) M. B. Dowell, Ph.D. Dissertation, The Pennsylvania State University, 1967; M. B. Dowell, C. A. Hultman, H. R. O'Neal, and G. M. Rosenblatt, paper in preparation.

(17) C. A. Hultman, Ph.D. Dissertation, The Pennsylvania State University, 1975.

(9) G. M. Rosenblatt, *J. Chem. Phys.*, in press.

(10) P. K. Lee and G. M. Rosenblatt, *J. Chem. Phys.*, **49**, 2995 (1968).

(11) R. Hultgren, P. D. Desai, D. T. Hawkins, M. Gleiser, K. K. Kelley, and D. D. Wagman, "Selected Values of the Thermodynamic Properties of the Elements", American Society for Metals, Metals Park, Ohio, 1973.

(12) J. J. Murray, C. Pupp, and R. F. Pottier, *J. Chem. Phys.*, **58**, 2569 (1973); **59**, 4572 (1973).

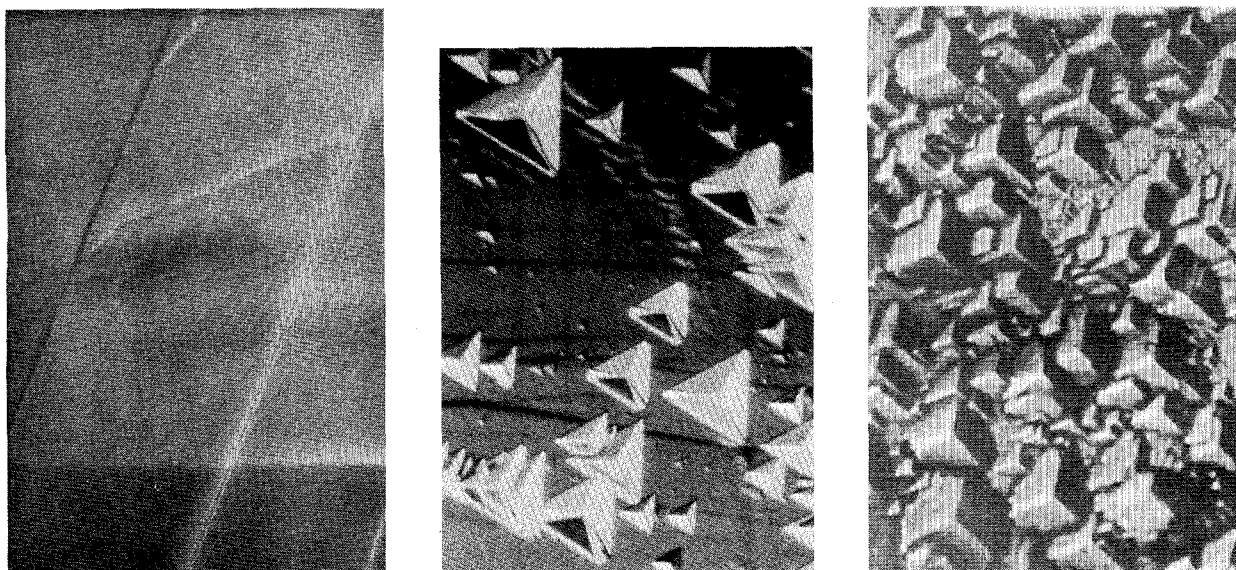


Figure 2. Photomicrographs of vaporizing As(111) surfaces: (a, left) fresh cleaved (phase contrast, 330 $\times$ ), (b, middle) during induction period (interference contrast, 360 $\times$ ), (c, right) at steady-state (brightfield, 690 $\times$ ). (The photographs are of different surfaces.)

other investigators to produce pits at dislocations.<sup>16</sup> Vaporization etch pits are trigonally symmetric on As(111),<sup>16-18</sup> which implies that they form at screw dislocation lines along the [111] direction,<sup>19</sup> whereas many chemical etch pits are asymmetric.<sup>19</sup> More detailed comparisons of vaporization and chemical etch pits, after different surface preparations and impurity exposures, show that vaporization pits do not usually form at all screw dislocations and that the appearance of pits at dislocations is affected by impurities.<sup>17,18</sup>

Figure 3 is a plot of the dimensions of a typical triangular pit as a function of time.<sup>16</sup> As the figure illustrates, pits normally grow outwards at a constant rate.<sup>14-17</sup> In addition to triangular pits, shallow, flat-bottomed pits, which are observable only using interference contrast techniques, appear on the background flat surface upon initial vaporization of freshly cleaved, unannealed samples (see upper left corner of Figure 2b). Flat-bottomed pits are not seen on annealed samples. The shallow, flat-bottomed pits grow at a rate  $\frac{1}{4}$ th to  $\frac{1}{14}$ th that of the growth rate of normal pyramidal pits.<sup>18</sup> Pit shapes and growth rates are affected by impurities.<sup>15-18</sup>

**Rate Changes.** During the initial stages of vaporization, while triangular pits are growing and before they intersect, the vaporization rate increases. This kinetic induction period may be seen in Figure 4, in which measured rates are plotted according to eq 4. The first few data points are below the steady-state Arrhenius or Clapeyron line and approach it consecutively. The plot shows two crystal samples; the dislocation density of one has been reduced significantly by cleaving at liquid-nitrogen temperature, rather than at room temperature. Reducing the dislocation density reduces the pit density and both lowers the initial rate and causes the induction period to be extended. However, the steady-state rate attained when the surface is covered by intersecting pits is independent of dislocation and pit densities.

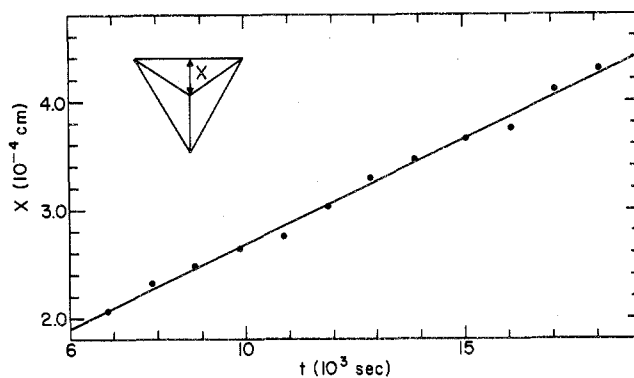


Figure 3. Growth of an arsenic vaporization pit at 260  $^{\circ}$ C. (The oscillations correspond to temperature fluctuations in the experiment.)

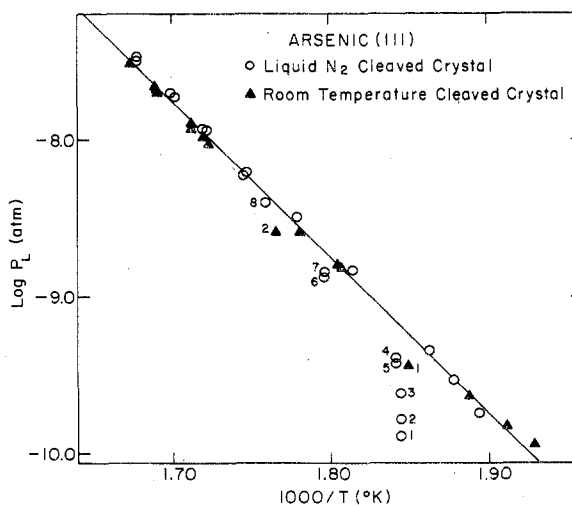
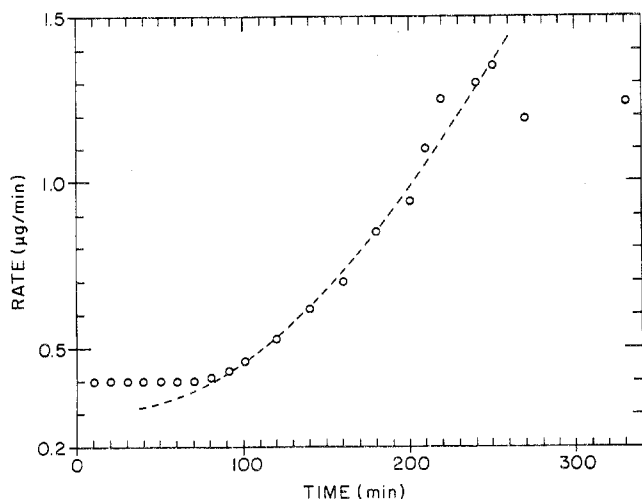


Figure 4. Vaporization rate as a function of temperature for two As(111) surfaces. The liquid-nitrogen-cleaved crystal has a significantly lower dislocation density. The points are numbered in the order in which they were taken. See eq 2 and 4 for the meaning of  $P_L$ .

The time dependence of the initial rate of the liquid-nitrogen-cleaved crystal is shown in Figure 5 and discussed further below.

(18) C. A. Hultman and G. M. Rosenblatt, *Science*, 188, 145 (1975).

(19) M. N. Shetty and J. B. Taylor, *J. Appl. Phys.*, 39, 3717 (1968).



**Figure 5.** Vaporization rate as a function of time upon initial vaporization of the liquid-nitrogen-cleaved crystal in Figure 4;  $T = 542$  K. The steady-state rate at this temperature is  $2.2 \mu\text{g}/\text{min}$ . The dashed line represents a parabolic rate increase.

### Molecular Interpretation

**Terraces, Ledges, Kinks, and Dislocations.** Kossel<sup>20</sup> and Stranski<sup>21</sup> suggested in the 1920's that atomization occurs by the stepwise mechanism illustrated in Figure 6, since there is insufficient energy available for atoms in a perfect surface to dissociate directly into the vapor. Observations during the intervening years have led to wide acceptance of their terrace-ledge-kink model.<sup>2-6</sup> In this model, atoms leave a crystal by dissociating from ledges (or steps) at kinks (or jogs), then diffusing on the terrace, then desorbing. When an atom leaves a kink, the kink moves but is conserved. Similarly, when a kink passes a given point on the ledge, the ledge moves. Thus, many theoretical discussions of vaporization, and of related processes, are concerned with ledge and kink dynamics.<sup>3,22,23</sup>

Frank<sup>22</sup> pointed out the importance of dislocations as ledge sources. Screw dislocations (which correspond conceptually to cutting into the crystal up to the dislocation line, then shearing one side of the cut with respect to the other a distance of one or more atomic layers until the crystal is in match again) result in a ledge on a surface intercepted by the dislocation line. Such ledges may act as vaporization sources, or crystal growth sinks, forming vaporization pits, as illustrated in Figure 7, or growth spirals.<sup>3,22</sup>

The triangular pits which appear on As(111) surfaces have the characteristics expected of spiral vaporization pits at screw dislocations<sup>17-19</sup> (see preceding section describing observed surface features). From the layered, crystal structure of arsenic shown in Figure 1, the minimum height of a ledge is one-third of the  $c$  axis of the rhombohedral unit cell,  $3.5 \text{ \AA}$ . Monomolecular ledges of minimum height are in accord with low-energy electron diffraction observa-

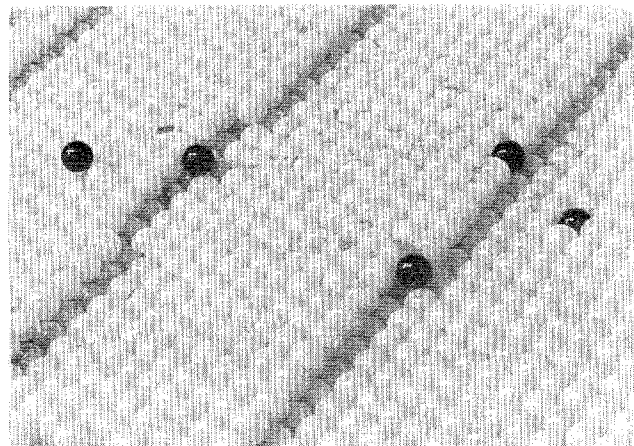


**Figure 6.** Marble model of the (111) face of a fccub crystal. Black atoms, from right to left, illustrate successive stages upon evaporation from the bulk (12 nearest neighbors  $n$ ) to the vapor ( $n = 0$ ); atom in surface ( $n = 9$ ), atom in ledge ( $n = 7$ ), kink atom (half-crystal position,  $n = 6$ ), atom adsorbed at ledge ( $n = 5$ ), atom adsorbed on surface at potential minimum ( $n = 3$ ).

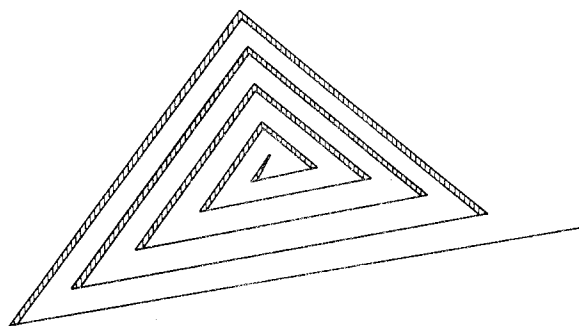


**Figure 7.** Schematic drawing of triangular vaporization pit at a screw dislocation.

tions on arsenic.<sup>24</sup> Assuming monomolecular ledges, the average pit slope of  $11^\circ$  corresponds to an average spacing  $\lambda$  between ledges of  $18 \text{ \AA}$ .

**Possible "Rate-Limiting" Steps.** We anticipated that, when  $\alpha_v \approx 10^{-4}$ , the impediment to vaporization might occur primarily in a single step of the vaporization sequence. Arsenic vaporization could be retarded by slow desorption of mobile  $\text{As}_4$  molecules, by slow surface diffusion away from ledges, by an activation energy barrier to formation of  $\text{As}_4$  molecules from crystal atoms at kinks, or by energy barriers to kink formation. (There are no indications that As atoms or  $\text{As}_2$  molecules play a role in the vaporization of  $\text{As}_4$ <sup>17</sup> and the energetics of the system<sup>11,12</sup> make their participation improbable.)

The observations that vaporization rates increase with time and that initial rates depend upon dislocation density show that the rate depends upon the concentration of sites at which molecules are formed on the crystal surface. These observations, as well as the temperature dependence of the steady-state rate,<sup>9,10</sup> imply that vaporization is not retarded simply by the rate of desorption of mobile  $\text{As}_4$  molecules, as it might be if, for example, a specific orientation of the tetrahedral molecule were required for desorption.<sup>25</sup>

Surface diffusion may become rate limiting when surface migration is slow compared to the surface res-

(20) W. Kossel, *Nachr. Ges. Wiss. Göttingen, Math.-Phys. Kl.*, 135 (1927); *Ann. Phys.*, **33**, 651 (1938).

(21) I. N. Stranski, *Z. Phys. Chem.*, **136**, 259 (1928); *Z. Phys. Chem., Abt. B*, **11**, 421 (1931).

(22) F. C. Frank, *Discuss. Faraday Soc.*, **5**, 48, 67 (1949); W. K. Burton, N. Cabrera, and F. C. Frank, *Philos. Trans. R. Soc. London, Ser. A*, **243**, 299 (1951).

(23) T. Surek, J. P. Hirth, and G. M. Pound, *J. Chem. Phys.*, **55**, 5157 (1971); *Surf. Sci.*, **41**, 77 (1974).

(24) J. W. Tester, C. C. Herrick, and W. P. Ellis, *Surf. Sci.*, **41**, 619 (1974).

(25) E. M. Mortenson and H. Eyring, *J. Phys. Chem.*, **64**, 846 (1960).

idence time.<sup>3,23</sup> For arsenic, surface diffusion seems an unlikely rate-limiting process since As<sub>4</sub> is estimated to be bound to the As(111) surface, which is atomically quite smooth, with an energy in the range of 10–20 kcal.<sup>26</sup> All experimental and theoretical indications are that As<sub>4</sub> has a reasonably long residence time on As(111), that As<sub>4</sub> migrates relatively freely on arsenic(111) and similar surfaces, and that As<sub>4</sub> desorbs from the surface randomly, in thermal equilibrium with the surface.<sup>26–30</sup> With arsenic, in contrast to KCl, for example, pit slopes do not change as one proceeds outwards from the spiral ledge source,<sup>13</sup> as they might if surface diffusion constraints controlled the vaporization kinetics.<sup>3,23</sup>

A more likely possibility<sup>2</sup> is that the rate is limited by the rate at which As<sub>4</sub> molecules are formed at kinks. In this event, or if the rate-limiting step occurs even earlier in the stepwise reaction sequence (e.g., if it is kink formation), molecules are removed with equal probability from any given segment of a spiral ledge. It follows that all the ledges on the sides of a pit will move at equal velocities. Thus, pit slopes will be independent of the distance from the pit center and independent of time (assuming there are no impurity perturbations), as observed. The pit slopes presumably reflect the ledge spacing initially established in the distorted region of the crystal near the screw dislocation line.

When vaporization is limited by the rate at which molecules are detached from ledges, or by earlier steps in the stepwise sequence, the vaporization rate will be proportional to the total length of ledge on the surface. If the number of active dislocations is varied, the initial time-dependent rate, while the surface contains individual, growing pits (Figure 2b), will change with the pit (and dislocation) density. Figure 4 shows that appreciably more time, and appreciably greater mass loss, elapse before steady state is attained with a low-dislocation-density, liquid-nitrogen-cleaved crystal, than with a crystal cleaved at room temperature. Furthermore, if the rate is proportional to ledge length and if pits have constant slope, one expects the vaporization rate to be constant after the surface is covered by intersecting pits (Figure 2c). After intersection, the length of ledge on the surface is determined solely by the average spacing,  $\lambda$ , between ledges, which in turn depends upon average pit slopes, but not upon the number of dislocation ledge sources. Figure 4 illustrates that the steady-state rate is independent of dislocation density.

These indications that the vaporization rate is proportional to the ledge length led to further consideration of the implications of such a mechanism and to measurement of ledge velocities.

**Rates of Vaporization and of Pit Growth during the Kinetic Induction Period.** Consider an evaporation pit with a spiral ledge structure such as that illustrated in Figure 7. If the ledges are, on the

average, a constant distance  $\lambda$  apart and if the vaporization rate is proportional to the ledge length, the rate will be proportional to the projected area of the pit. Furthermore, the vaporization rate from unit area of pitted surface will equal the steady-state Langmuir vaporization rate,  $r_L$ , from the intersected surface. Thus, the instantaneous vaporization rate from one pit is

$$dw_P/dt = r_L(3)^{3/2}x^2 \quad (6)$$

where  $x$  is defined in Figure 3. The mass loss that has occurred from the pit at time  $t$  is given by the product of the pit volume and the crystal density,  $d$

$$w_P = d\sqrt{3}(\tan \theta)x^3 \quad (7)$$

where  $\theta$  is the angle between the pit side and the (111) surface. Differentiation of eq 7 with respect to time and comparison with eq 6 yield the rate of growth of a pit side

$$dx/dt = r_L/d \tan \theta \quad (8)$$

Under the conditions assumed here (but see below),  $dx/dt$  equals the ledge velocity.

Integrating eq 8 from  $x = 0$  at  $t = 0$  and substituting into eq 6 give the rate of vaporization during the induction period, before pits start to intersect, for a crystal of pit density  $\eta$ .

$$\frac{d(w/A)}{dt} = \frac{(3)^{3/2}\eta}{(d \tan \theta)^2} r_L^3 t^2 \quad (9)$$

The above analysis assumes that all pits start to grow at the same time and that they grow at the same rate so that pits are all the same size. In actuality (see Figure 2b), the time of pit initiation and the rate of pit growth are affected markedly by point defects (vacancies and impurities), as are pit shapes.<sup>15–18</sup> The analysis also assumes that no vaporization occurs from surface area not covered by pyramidal pits. However, the surface region between pyramidal pits contains cleavage steps, as well as ledges from shallow, background, flat-bottomed pits. The background surface evaporates at a lower, but often noticeable, rate,  $r_0$ . If this rate is included in the analysis,  $r_L$  in eq 8 and 9 should be replaced by  $r_L - r_0$ , and  $r_0$  should be added to the right side of eq 9.

Equation 8 implies that plotting pit dimensions  $x$  as a function of time will yield straight lines. This is observed<sup>13–18</sup> (see Figure 3). Equation 8 further implies that the pit growth rates represented by the slopes of these lines can be calculated from steady-state vaporization rates  $r_L$  and from pit angles  $\theta$ . Comparisons of observed:calculated growth rates for triangular pits in the author's laboratory<sup>16,17</sup> yield ratios covering the range 0.4 to 7.0 with an average value of 3.9. Independent measurements by Tester, Herrick, and Reid<sup>15</sup> yield ratios in the range 0.2–0.7. The agreement is probably as good as can be expected considering experimental and sampling errors and the known effects of impurities and residual gas on pit growth rates and shapes.<sup>15–18</sup>

Equation 9 indicates that a plot of vaporization rate vs.  $t^2$  during the induction period should be a straight line. Such a plot has been made for the data in Figure 5. The straight line obtained is plotted as a parabolic dashed line in Figure 5. The slope of the

(26) S. B. Brumbach and G. M. Rosenblatt, *Surf. Sci.*, **29**, 555 (1972).

(27) J. R. Arthur, *J. Appl. Phys.*, **37**, 3057 (1966).

(28) B. C. Martin and G. M. Rosenblatt, *J. Cryst. Growth*, in press.

(29) M. Balooch, A. E. Dabiri, and R. E. Stickney, *Surf. Sci.*, **30**, 483 (1972).

(30) R. S. Lemons, Ph.D. Dissertation, The Pennsylvania State University, 1974.

line representing rate vs.  $t^2$  is one-half of that computed from eq 9. If the deviation is used to estimate the vaporization rate,  $r_0$ , from the unpitted portions of the surface for this liquid-nitrogen-cleaved, unannealed crystal (by replacing  $r_L$  in eq 9 by  $r_L - r_0$ ), one obtains  $r_0 \approx 0.2r_L$ . The estimate agrees with the value obtained by direct comparison of the measured initial rate with the steady-state rate  $r_0/r_L = 0.4/2.2 = 0.18$ . The value of  $r_0$  obtained from weight-loss measurements is in general accord with the observation that background, flat-bottomed pits on unannealed samples grow outwards at rates  $1/4$ th to  $1/14$ th that of pyramidal pits.<sup>18</sup>

As Figure 5 illustrates, there are four stages in the vaporization of a freshly cleaved arsenic crystal. First, the crystal evaporates at a constant rate. During this period most of the evaporation comes from cleavage steps and disturbed portions of the unpitted surface. Next, there is a stage of parabolic growth, where ledges from dislocations dominate and most of the vaporization comes from individual triangular pits. The rate stops increasing rapidly as pits start to intersect. The rate finally reaches steady state when the surface is completely covered by intersecting pits. The initial rate,  $r_0$ , is sensitive to the dislocation density and the previous history of the sample. The rate during the parabolic rate increase is proportional to the density,  $\eta$ , of vaporization pits. Assuming a reasonably uniform pit density, the time and mass loss required to reach steady state goes as  $1/\eta^{1/2}$ .<sup>14</sup> However, the steady-state rate,  $r_L$ , is independent of the pit and dislocation density.

### Mechanism of Arsenic Vaporization

**"Picture" of the Molecular Mechanism.** The experiments and analysis summarized in the preceding sections have shown that the rate of arsenic vaporization is proportional to the length of ledge on the surface, that the primary sources of ledges are screw dislocations, and that  $\text{As}_4$  molecules, after they are formed at ledges, migrate on the surface and desorb randomly in thermal equilibrium with the solid. The results do not establish whether the rate-determining step is atomic rearrangement to form  $\text{As}_4$  molecules at kinks on ledges or an earlier step in the reaction.

Very recent investigations, based upon and similar in approach to those recounted here, indicate that arsenic vaporizes by a "zipper", or unraveling, mechanism.<sup>18</sup> The process is a three-dimensional analogue of the zipper mechanisms which describe reactions of chainlike high polymers. Arsenic vaporization is initiated by formation of a kink at the origin of a spiral ledge at the center of a vaporization pit (see Figure 7). The pit center corresponds to the perturbed crystal region where the screw dislocation line intersects the surface. Not surprisingly, kink formation at the ledge origin is very sensitive to impurities and vacancies (i.e., point defects).<sup>17,18</sup> In the "zipper" model, after being formed, a kink moves outwards rapidly along the ledge by releasing  $\text{As}_4$  molecules (analogous to the slider on a zipper). Thus, the number of gaslike  $\text{As}_4$  molecules ejected by a kink is proportional to the length of ledge which the kink traverses. It follows that, if kinks are initiated at a constant rate, ledges move at a constant rate, so the observed evap-

oration rate will be proportional to the length of ledge.

Qualitative indications of this mechanism come from further investigation of the shape, location, and crystallographic orientation of vaporization etch pits.<sup>18</sup> The mechanism is in accord with the observation that changes in pit slopes or shapes start from pit centers and propagate outward.<sup>18</sup> Some of these changes move more rapidly than do ledges or pit edges.<sup>18</sup> It has been observed that a surface cut at an angle of  $11^\circ$  to (111) rearranges further upon vaporization.<sup>24</sup> Quantitative information comes from measurements of the velocity at which changes in pit slopes and pit shapes are propagated.<sup>17,18</sup> (These changes occur when point defects interact with dislocations.) At  $293^\circ\text{C}$ , where the steady-state vaporization rate is  $10^{14}$  molecules  $\text{cm}^{-2} \text{s}^{-1}$ , measured ledge velocities of  $\sim 10^{-6}$  cm  $\text{s}^{-1}$  show kinks to be initiated at a rate of about  $10 \text{ s}^{-1}$  per dislocation. Combining this result with measured kink velocities of  $\sim 0.1$  cm/s one finds that a kink releases, on the average, almost  $10^6$   $\text{As}_4$  molecules, moving more than  $10^6 \text{ \AA}$  along the ledge, before the next kink is initiated.<sup>18</sup>

**Implications and Future Directions.** This report illustrates how kinetic studies of reaction rate and of changes in surface topography can lead to a detailed, molecular interpretation of a stepwise surface reaction. (This does not imply that there is not more to be learned.) This discussion has been restricted to the retarded vaporization of arsenic. However, one obviously wonders in what way the results described here may be applied to other surface reactions of arsenic, to surface reactions in chemically similar systems, to vaporization of rather different chemical systems, and, most interesting of all, to research in other areas of surface science. The answers, of course, are the subject of future experimentation.

It is clear that the results described here have rather direct implications for the vaporization and crystal growth of other elemental systems forming molecular vapors,<sup>13</sup> for "catalysis"<sup>6,8</sup> of retarded vaporization, and for other vaporization, condensation, and gas-surface reactions dominated by screw dislocations.<sup>9,28</sup> It is also clear that elucidation of surface reaction paths is enhanced by, indeed requires, the combined use of complementary experimental techniques. The chemical and molecular interactions alluded to here will, no doubt, be clarified a great deal by such surface probes as LEED (low-energy electron diffraction), Auger, ESCA (electron spectroscopy for chemical analysis) and molecular beam scattering.

To proceed further, one can only conjecture. It was pointed out in the introduction that the vaporization of arsenic is a chemical reaction in which atoms arranged in a layered crystalline array undergo extensive electronic and geometric rearrangement to form individual tetrahedral molecules. The observations summarized here show the important role played by defects, and by interactions between defects, in this chemical rearrangement. The reaction utilizes and is affected by both surface defects, i.e., ledges and kinks, and crystal defects, i.e., dislocations, impurities, and vacancies. I anticipate that defects will dominate most chemical reactions which occur at solid surfaces; indeed, it is difficult to overemphasize



their importance. In this sense, the results from the vaporization of arsenic bear more closely upon gas-surface reactions, corrosion, dissolution, heterogeneous catalysis, and retarded sublimation, than they do upon "normal" sublimation ( $\alpha_v^\circ \approx 1$ ) or the vaporization of liquids. It is fascinating that recent studies of catalysis using single crystals<sup>31</sup> show that, although heterogeneous chemical reactions do not occur on low-index surface planes, they do take place at ledges and kinks similar to those which play such

(31) G. A. Somorjai and L. L. Kesmodel, *MTP Int. Rev. Sci.*, in press. G. A. Somorjai, *Proc. Battelle Conf. Heterogeneous Catal.*, in press.

an important role in retarded molecular vaporization.

The author is indebted to Michael B. Dowell, Carl A. Hultman, and H. R. O'Neal for their substantial contributions to the research summarized here. The work was sponsored by the National Science Foundation (Grant MPS 75-04801) and by the Army Research Office, Durham. This account was written while the author was a guest scientist at the Inorganic Materials Research Division, Lawrence Berkeley Laboratory, University of California. The author gratefully thanks the U.S. Energy Research and Development Administration and the Lawrence Berkeley Laboratory for their support and assistance and Alan W. Searcy for helpful comments on the manuscript.

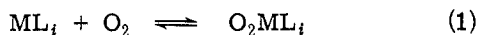
## Dioxygen-Metal Complexes: Toward a Unified View<sup>1</sup>

Lauri Vaska

Department of Chemistry, Clarkson College of Technology, Potsdam, New York 13676

Received February 4, 1975

This Account is concerned with the question of the nature of dioxygen bound to the metal atom in a molecular compound, and some consequences arising from these observations. This question is important not only in its own right but also because it must be answered before one can hope to understand the factors which influence the reversible oxygenation of metal complexes (eq 1), notably hemoglobin and re-



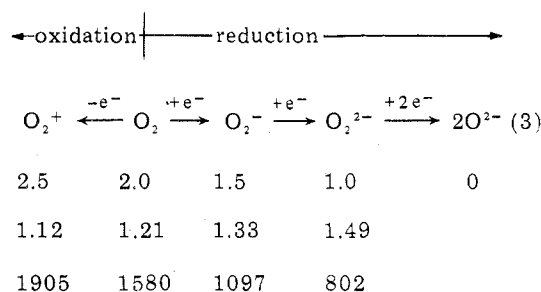
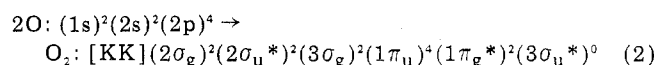
M = central metal atom;  $L_i$  =

"permanent" (auxiliary) ligands

lated hemoproteins, which continue to provide a primary inspiration for the study of the title compounds.

Several reviews of dioxygen-metal complexes,  $O_2ML_i$ , have appeared in recent years,<sup>2</sup> and countless other papers and books contain analogous review type material. These writings, however, have mainly been confined to certain types of dioxygen compounds, compilations of data, or citations from articles preceding them. The present Account has thus been prompted by a need for an overall and reasonably current version of the subject, and also to show that some data which have been considered representative<sup>3</sup> have become exceptions.

Some properties and reactions of molecular oxygen pertinent to the discussion of dioxygen-metal complexes are summarized below. The ground-state electronic structure is given in eq 2, and eq 3 schemati-



(1) Some terminology used in this paper: (a) dioxygen—generic designation of diatomic oxygen ( $O_2$ ); it comprises all states and forms of  $O_2$  in which there is an "oxygen-oxygen covalent bond", regardless of whether dioxygen is free, part of another compound, or carries an electronic charge, etc; (b) dioxygen-metal complex—includes one or more covalent bonds between dioxygen and metal atom(s) in a molecular unit, without further specification of bonding and structure; (c) molecular oxygen—free or isolated neutral  $O_2$ ; refers usually to the ground-state configuration, but does not exclude other states of the molecule; (d) superoxide— $O_2^-$  ion; superoxo—covalently bound dioxygen resembling  $O_2^-$ ; superoxo-metal complex: contains metal-bound superoxo ligand(s); (e) peroxide— $O_2^{2-}$  ion; peroxo—covalently bound dioxygen resembling  $O_2^{2-}$ ; peroxo-metal complex—contains metal-bound peroxo ligand(s); (f) oxide— $O^{2-}$  ion; oxo: covalently bound monatomic oxygen resembling  $O^{2-}$  (the term dioxo,  $(O)_2$ , is not to be confused with dioxygen,  $O_2$ ); (g) oxygenation—dioxygen (usually molecular  $O_2$ ) addition; deoxygenation—dioxygen (usually molecular oxygen) subtraction from a dioxygen compound; (h) dioxygen carrier or dioxygen-carrying compound, = oxygen carrier—refers to dioxygen transport by a (metal) compound, i.e., uptake, transport, release. This process, specifically a biological one, is also called reversible oxygenation, which is a more general chemical term (eq 1); (i) oxygen—generic term for the element and its various forms; since it is widely used for several oxygen species, it cannot be avoided as a synonym for some of the terms cited above.

(2) (a) L. H. Vogt, Jr., H. M. Faigenbaum, and S. E. Wiberley, *Chem. Rev.*, **63**, 269 (1963); (b) J. A. Connor and E. A. V. Ebsworth, *Adv. Inorg. Chem. Radiochem.*, **6**, 279 (1964); (c) E. Bayer and P. Stretzmann, *Struct. Bonding*, **2**, 181 (1967); (d) A. G. Sykes and J. A. Weil, *Prog. Inorg. Chem.*, **13**, 1 (1970); (e) R. Wilkins, *Adv. Chem. Ser.*, No. 100, 111 (1971); (f) V. J. Choy and C. J. O'Connor, *Coord. Chem. Rev.*, **9**, 145 (1972/73); (g) J. Valentine, *Chem. Rev.*, **73**, 235 (1973); (h) L. Klevan, J. Peone, Jr., and S. K. Madan, *J. Chem. Educ.*, **50**, 670 (1973); (i) G. Henrici-Olivé and S. Olivé, *Angew. Chem., Int. Ed. Engl.*, **13**, 29 (1974).

Lauri Vaska was born in Rakvere, Estonia. He attended the Baltic University in Hamburg and the University of Göttingen in Germany in 1946–1949, and obtained his Ph.D. from the University of Texas with Professor George W. Watt in 1956. After a postdoctoral year at Northwestern University with Professor P. W. Selwood, he was a Fellow of Independent Research at Mellon Institute until 1964, when he joined the faculty at Clarkson College of Technology, where he is Professor of Chemistry.